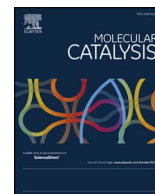




Contents lists available at ScienceDirect

## Molecular Catalysis

journal homepage: [www.elsevier.com/locate/mcat](http://www.elsevier.com/locate/mcat)

# Ordered mesoporous $\gamma$ -Al<sub>2</sub>O<sub>3</sub> as highly efficient and recyclable catalyst for the Knoevenagel reaction at room temperature

Piyali Bhanja, Utpal Kayal, Asim Bhaumik\*

Department of Materials Science, Indian Association for the Cultivation of Science, Jadavpur, Kolkata, 700 032, India

## ARTICLE INFO

## Keywords:

Knoevenagel condensation  
Mesoporous alumina  
Coumarin-3-carboxylic acid  
Surface acidity and basicity  
C–C bond formation and cyclization

## ABSTRACT

Coumarins are important class of organic compounds and intensively used in agricultural and pharmaceutical industries. We have developed a strategy for the synthesis of coumarin derivatives quantitatively via Knoevenagel condensation reaction of an *ortho*-hydroxyaryl aldehyde and an activated methylene compounds in the presence of ordered mesoporous  $\gamma$ -Al<sub>2</sub>O<sub>3</sub> as a heterogeneous catalyst. The catalyst has been thoroughly characterized through powder X-ray diffraction, N<sub>2</sub> sorption analysis, FTIR spectroscopy, TG/DTA, NH<sub>3</sub>-TPD and CO<sub>2</sub>-TPD (temperature programmed desorption) analysis. The material possesses periodicity in mesopores and both surface acidic and basic sites having strengths of 1.47 and 1.11 mmol g<sup>-1</sup>, respectively, which is highly favorable for carrying out the Knoevenagel condensation reaction for the synthesis of a wide range of condensation product (yields ~98%) under very mild conditions. This amphoteric catalyst exhibits good surface Lewis acidity/basicity and high recyclability up to sixth reaction cycles without any significant loss in the product yield.

## 1. Introduction

Coumarins are very demanding class of heterocyclic organic compounds, employed in various application areas like perfumes, additives to optical brightening agents [1], cosmetics and foods [2], insecticides [3], fluorescent dyes [4], triplet oxygen sensitizers [5] and laser dyes [6] etc. Naturally, coumarins are extracted from the routes, leaves and seeds of plant resources. Acenocoumarol, dicoumarol, warfarin are important coumarin derivatives having a wide spread pharmaceutical importance like antioxidant [7], antibacterial [8], antifungal [9], anti-HIV [10], analgesic [11], antibiotic [12], anticancer [13], antitumor [14] and also used as an anticoagulant [15]. Thus, synthesis of coumarins and its congener through an effective and environmentally benign approach is very essential. The potential of coumarins were first evolved in mind 18th century with perkins reaction and still preferred now-a-days to prepare its few simple derivatives [16]. Coumarin based heterocyclic compounds like coumarin-3-carboxylic acid are used in semisynthetic pharmacological agents like tetrahydropyridones [17,18], isoureas [19] and  $\beta$ -lactams [20]. Coumarine derivatives bearing carboxylic acid at 3-position are synthesized through the Knoevenagel condensation reaction since early 90s'. By employing, Reformatsky [21], Pechmann [22] and Wittig reactions [23] coumarin derivatives are now being synthesized conventionally. Although the synthesis of coumarin derivatives are conducted in a straight forward

way through these methods, adverse reaction conditions and hazardous non-ecofriendly solvents are the major drawbacks of this process [24]. Condensation of aldehydes with active methylene compounds to form C–C bond in organic synthesis (Knoevenagel condensation) have a wide spread impact in various applications like heterocyclic Diels-Alder reaction [25], preparing several biologically active heterocyclic compounds [26] as well as carbocyclic compounds of biologically important value added intermediate products for anti-hypertensive drugs and calcium antagonist [27]. Knoevenagel condensation generally involves the introduction of conjugated double bonds in aromatic compounds using a solid basic catalyst, such as alkali or alkaline earth metal oxides as catalyst. Usually, basic surfaces of molecules like ammonia, sodium ethoxide and amines can catalyze this reaction in the presence of organic solvents [28,29]. Further, zeolites [30], various Lewis acids [31], ionic liquids [32] are also used as good heterogeneous catalyst for this reaction. Brahmachari have reported one-pot synthesis of coumarin-3-carboxylic acids over homogeneous catalytic system K<sub>2</sub>CO<sub>3</sub> or NaN<sub>3</sub> at room temperature [33]. However, the reaction takes very long time to reach optimum conversion (20 h) and the catalysts are not recyclable. Use of heterogeneous solid bases in comparison to its homogeneous counter-part is highly recommended in this context owing to a number of efficacious effects like simplicity of reaction process, less corrosiveness, reusability with high turn-over number and ease of catalyst recovery.

\* Corresponding author.

E-mail address: [msab@iacs.res.in](mailto:msab@iacs.res.in) (A. Bhaumik).<https://doi.org/10.1016/j.mcat.2018.01.019>Received 30 August 2017; Received in revised form 1 January 2018; Accepted 14 January 2018  
2468-8231/ © 2018 Elsevier B.V. All rights reserved.

Alumina is a widely studied metal oxide, which gained a considerable attention in chemical industry as adsorbent, catalyst, catalyst support, drying agent either alone or in the presence of other oxides [34–36].  $\gamma$ -alumina, the most well-known aluminum oxide phase has been studied intensively as catalyst in organic chemistry [37]. Compared to clays and zeolites, alumina does not have accessible reactive groups and cavities. However, due to the presence of electron deficient Al(III) sites together with surface basicity alumina are responsible for its broad spectrum of applications, viz. purification of ground water, automobile emission control, catalytic support in petroleum refining and so on [38]. Due to their high specific surface area with narrow pore size distribution, uniformity of pore channels and tunable pore diameter, mesoporous alumina [39,40] could be an ideal candidate in heterogeneous catalysis for the synthesis of various value added organic fine chemicals. Innovation of ordered mesoporous alumina with amorphous wall by a sol-gel approach under rigid hydrolysis process and condensation of reagents are documented by Somorjai et al. [41]. Zhang et al. recently proposed a new route of obtaining mesoporous alumina where they have innovated an ordered crystalline mesoporous alumina molecular sieves with CMK as hard template [42]. With the use of ionic liquids both as solvent and template Lian et al. evolved [43] a newer method, ionothermal synthesis to produce  $\gamma$ -Al<sub>2</sub>O<sub>3</sub> mesoporous nanoflakes. A ligand-assisted solvent evaporation induced co-assembly route is developed by Wei et al. for synthesizing the ordered mesoporous alumina (OMA) with an ultra large pore size using a high molecular-weight poly(ethylene oxide)-b-polystyrene (PEO-b-PS) as a soft template, aluminum acetylacetonate as a precursor and tetrahydrofuran as a solvent [44]. Weinberger et al. reported the synthesis of mesoporous alumina using photo-cross-linked polydimethylacrylamide hydrogels as porogen matrices [45].

Herein, we report the synthesis of ordered mesoporous  $\gamma$ -Al<sub>2</sub>O<sub>3</sub> using P123 as a structure directing agent *via* evaporation-induced self-assembly (EISA) method [46] followed by calcination and explored its catalytic activity. The material exhibits high surface acidic and basic sites together, thermal stability and considerably good surface area. Being amphoteric in nature the mesoporous  $\gamma$ -Al<sub>2</sub>O<sub>3</sub> material acts as a heterogeneous bi-functional catalyst for the Knoevenagel condensation reactions and for the synthesis of coumarin-3-carboxylic acid with excellent product yields.

## 2. Experimental section

### 2.1. Chemicals

Pluronic P123 (Poly(ethylene glycol))-block-poly(propylene glycol)-block-poly(ethylene glycol) ( $M_{n,v} = \sim 5800$ ) and aluminum isopropoxide ( $M_w = 204.24$  g/mol) were obtained from Sigma Aldrich, India. Citric acid ( $M_w = 192.123$  g/mol) and hydrochloric acid were purchased from Merck, India. All other organic solvents were used in catalytic reactions without further purification.

### 2.2. Synthesis method of mesoporous alumina (MPA-1)

In particular synthetic procedure, at first 2.0 g of structure directing agent P123 was dissolved in 40 mL absolute ethanol. 3.2 g of 37 wt% hydrochloric acid was added to the reaction mixture and followed by addition of 1.0 g of citric acid. After continuous stirring for 1 h 4.0 g of aluminum isopropoxide was added to the solution and allowed to vigorous stirring for 6 h until the white coloured gel was formed. Then the resulting viscous solution was subjected to keep inside the 60 °C oven for 60 h for slow evaporation reaction method. After drying the sample white solid was calcined at 500 °C and 1000 °C temperature in aerobic condition for 4 h at temperature ramp of 10 °C/min, denoted by MPA-1 and MPA-2 respectively. The solid samples were subjected for thorough characterization. A schematic illustration for formation of MPA-1 has been shown in Scheme 1.

### 2.3. Instrumentation

Small and wide angle powder X-ray diffraction patterns of MPA-1 and MPA-2 were recorded using Bruker D8 Advance SWAX diffractometer operated at voltage of 40 kV and current 40 mA. With a standard silicon sample the instrument was calibrated, using Ni-filtered Cu K $\alpha$  ( $\lambda = 0.15406$  nm) radiation. By employing Quantachrome Autosorb 1-C surface area analyzer nitrogen adsorption-desorption isotherms were obtained at 77 K. For gas adsorption purpose, the samples were degassed for 6 h at 453 K under high vacuum analysis. NLDFT (non local density functional theory) method has been employed for estimation of the pore size distributions from the nitrogen sorption isotherm. Using a Perkin-Elmer spectrum 100 spectrophotometer FTIR spectrum of the sample was recorded. Very small amount of solid sample was allowed to grind finely with a specially purified salt KBr to get rid of scattering effects from large crystals. Then the solid mixture was pressed by using mechanical press to obtain the translucent pellet and the pellet was subjected to keep inside the spectrophotometer for which the beam of the spectrometer can pass through. Thermogravimetric (TGA) and differential thermal analysis (DTA) of the mesoporous alumina samples were carried out in a TGA instrument thermal analyzer TA-SDT Q-600 under air flow. The temperature-programmed desorption of ammonia and CO<sub>2</sub> (NH<sub>3</sub>-TPD, CO<sub>2</sub>-TPD) experiments were performed on a flow apparatus (Micrometrics, ChemiSorb 2720). For the both experiments before taking that material in the U-type glass cell the sample was allowed to keep for outgassing at 130 °C temperature under inert atmosphere (helium) for 3 h. In case of NH<sub>3</sub>-TPD, after cooling down to room temperature, the ammonia (NH<sub>3</sub>) gas flow was started for 30 min at 30 mL/min to get the saturation condition and helium gas was purged again for 45 min to flush out the additional amount of NH<sub>3</sub> gas from the cell. Similar procedure was followed in case of CO<sub>2</sub>-TPD only after replacing the NH<sub>3</sub> gas flow by CO<sub>2</sub> through the samples. Then NH<sub>3</sub>-TPD and CO<sub>2</sub>-TPD desorption profile of this material are obtained using a thermal conductivity detector (TCD) while increasing the sample temperature at 5 °C/min ramp.

In a typical catalytic reaction, 1 mmol of substituted aromatic aldehyde and 1.1 mmol of malononitrile were dissolved into 25 mL round bottom (RB) flask containing 1 mL absolute ethanol. Then the reaction mixture was allowed to continuous stir for 20 min at room temperature when *p*-chlorobenzaldehyde was used as a model reaction. For different substrates reaction time varied from 7 to 120 min. For the acid hydrolysis of intermediate Knoevenagel product, 200 mg of 2-(2-hydroxybenzylidene)-malononitrile was taken into RB flask containing 10 mL water and three drops of 98% H<sub>2</sub>SO<sub>4</sub>. Then the reaction mixture was stirred continuously in preheated oil bath at 50 °C temperature for 1.5 h. The progress of the reaction was monitored through TLC and the product was confirmed through <sup>1</sup>H NMR and <sup>13</sup>C NMR in CDCl<sub>3</sub> solvent without any column purification. After catalytic reaction the products were identified using <sup>1</sup>H and <sup>13</sup>C NMR experiments using a Bruker DPX-300/500 NMR spectrometer.

## 3. Results and discussions

### 3.1. Nanostructure analysis

The small angle powder X-ray diffraction patterns of calcined samples MPA-1 and MPA-2 are shown in Fig. 1. The very sharp peak at  $2\theta$  value of 0.97° and low intense peak at  $2\theta$  value of 1.66° and 1.93° have been observed in small angle pattern of MPA-1 sample of Fig. 1a can be attributed to the 100, 110 and 200 planes of the 2D-hexagonally ordered mesophase. It is noticed that only one diffraction peak appears at  $2\theta$  value of 1.09° in Fig. 1b, suggesting the partial loss of periodicity of the mesopores in sample MPA-2 upon calcination of the as-synthesized material at 1000 °C. On the other hand the wide angle powder X-ray diffraction patterns of MPA-1 and MPA-2 samples are shown in

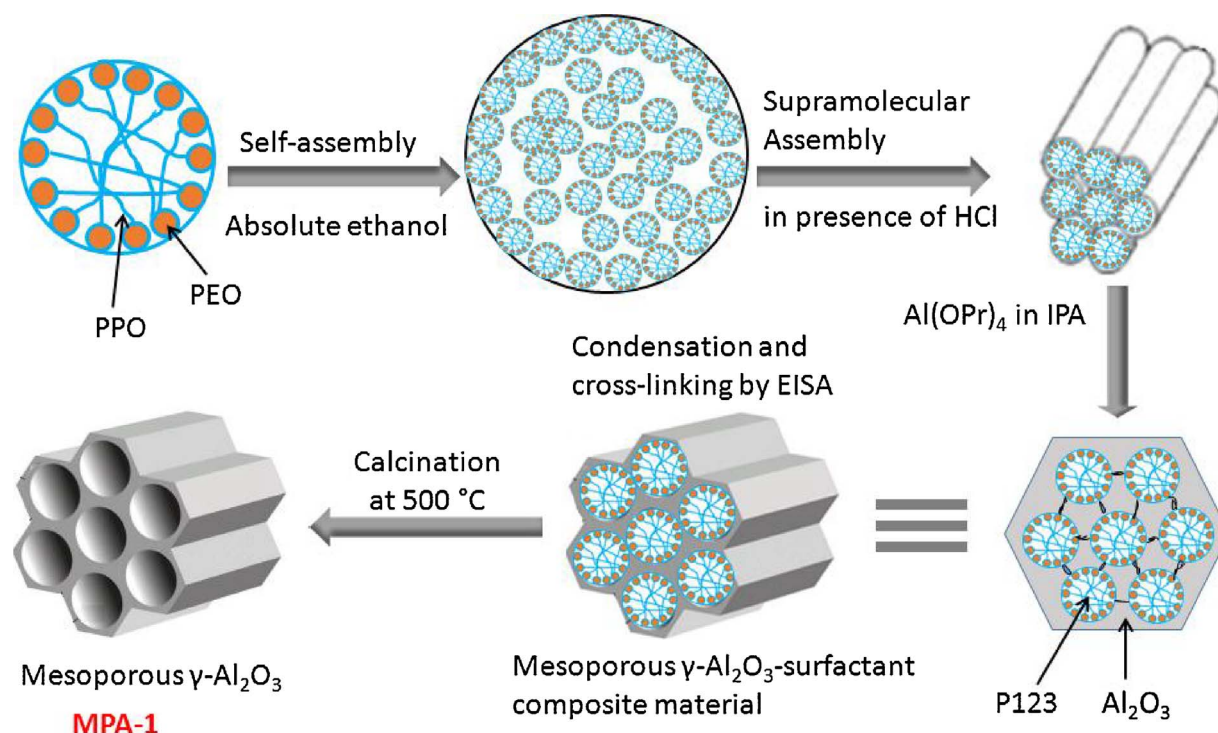
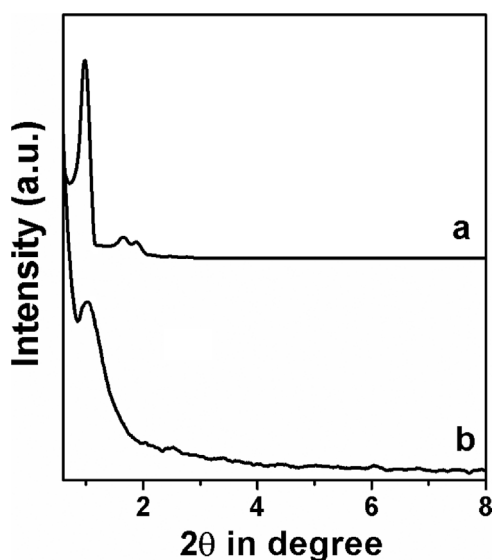
Scheme 1. Schematic representation for the synthesis of mesoporous  $\gamma$ -Al<sub>2</sub>O<sub>3</sub> (MPA-1).

Fig. 1. The small angle powder XRD pattern of MPA-1 (a) and MPA-2 (b).

Fig. 2. Very low intensity broad peaks are observed in case of MPA-1 sample, whereas highly crystalline and strong diffraction peaks is notified in the wide angle powder XRD pattern of MPA-2 sample. The latter diffraction pattern matched well with the phase of  $\gamma$ -Al<sub>2</sub>O<sub>3</sub> (JCPDS Card No. 10-0425). Thus, from this powder XRD data it can be concluded that with increasing the calcination temperature the mesopores are arranged in more disorder manner and pore walls are converted into a highly crystalline wall [46].

### 3.2. Surface area and porosity measurement

To measure surface area and porosity nitrogen sorption analysis has been carried out for both the calcined samples MPA-1 and MPA-2. Fig. 3Aa represents the nitrogen adsorption-desorption isotherm of MPA-1 samples, which showed typical type IV isotherm with a H1

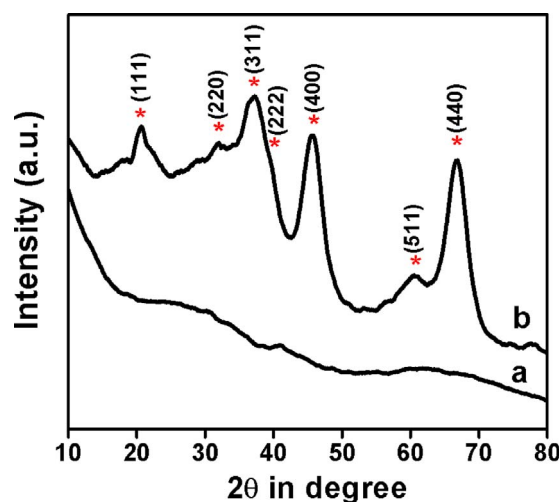


Fig. 2. The wide angle powder XRD pattern of MPA-1 (a) and MPA-2 (b).

hysteresis loop according to IUPAC nomenclature in the range of 0.60–0.83 relative pressure of nitrogen. The characteristic condensation in that particular  $P/P_0$  range suggests that the existence of mesopores throughout the samples. Fig. 3Ab displayed the nitrogen adsorption-desorption isotherm of MPA-2 sample and this isotherm can be classified as type IV isotherm with a broad hysteresis loop in  $P/P_0$  range of 0.60–0.90 relative pressure of nitrogen, suggesting the presence of wide range of mesoporosity in the material [47,48]. The BET (Brunauer-Emmett-Teller) surface areas of these samples were 415 and 223 m<sup>2</sup>g<sup>-1</sup>, respectively. Also, the pore volumes of the MPA-1 and MPA-2 materials were 0.5614 and 0.1879 ccg<sup>-1</sup>, repetitively. NLDFT method (non-local density functional theory) has been used to estimate the pore size distribution plots (Fig. 3Ba and Bb) and the pore size diameters of those above mentioned samples are obtained to be 6.2 nm and 5.0 nm, respectively. The De Boer statistical thickness (t-plot) indicates that surface area of MPA-1 sample is obtained 363 m<sup>2</sup>g<sup>-1</sup> due to mesoporosity and 53 m<sup>2</sup>g<sup>-1</sup> for microporous contribution to the total

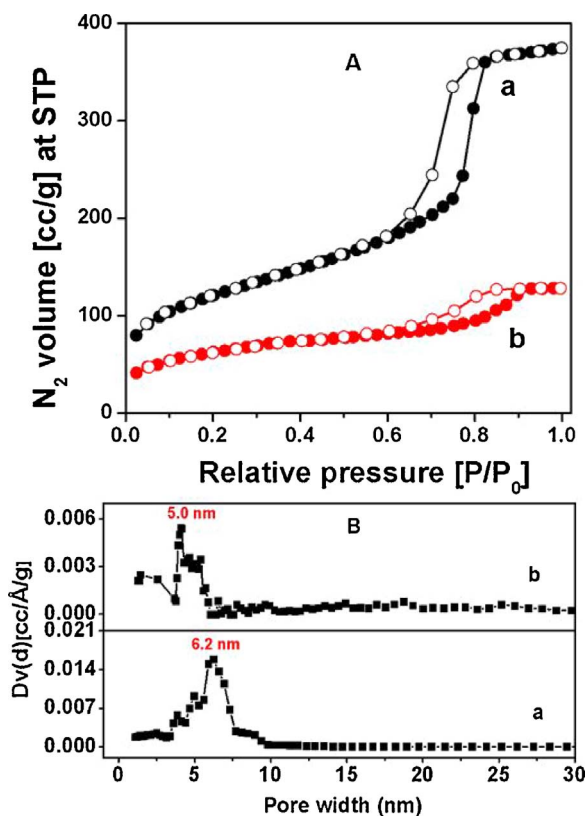


Fig. 3. (A) The  $N_2$  adsorption/desorption isotherm of MPA-1 (a) and MPA-2 (b). (B) The pore size distribution plots of MPA-1 (a) and MPA-2 (b) determined by using the NLDFT (Non Local Density Functional Theory) method.

surface area. Since MPA-1 sample possess higher surface area and pore volume than the MPA-2 sample the former has been employed as a heterogeneous catalyst for the synthesis of coumarin-3-carboxylic acids.

### 3.3. TEM analysis

The ultra-high resolution transmission electron microscopic images of MPA-1 are shown in Fig. 4a and b. As seen from Fig. 4a the uniform honeycomb like hexagonal array of ordered pores are seen throughout the whole specimen. The average pore width estimated from this image

is  $\sim 5.5$  nm. The FFT pattern shown in the inset of Fig. 4a suggested hexagonally ordered array of pores in the mesoporous  $\gamma$ - $Al_2O_3$  network. Further, in Fig. 4b the channel type arrangement of mesopores are clearly seen when seen along the perpendicular to the pore axis.

### 3.4. Spectroscopic analysis

FTIR spectrum of MPA-1 has been recorded in the spectral region of  $4000$ – $400$   $cm^{-1}$  and this is shown in Fig. S1 (ESI). Two peaks appeared at  $3452$  and  $1634$   $cm^{-1}$ , could be ascribed as the stretching and bending vibrations of hydroxyl ( $-OH$ ) groups, respectively. Further, two distinctive peaks at  $779$  and  $612$   $cm^{-1}$  could be assigned due to the existence of  $Al-O$  stretching vibration modes in  $AlO_6$  octahedra and  $AlO_4$  tetrahedra, respectively [49].

### 3.5. Thermal stability

To understand about the thermal stability of MPA-1 material we have carried out the thermal gravimetric analysis under air flow. Fig. S2a (ESI) represents the TGA plots of MPA-1 material where the first weight loss in the temperature region of  $85$ – $110$   $^{\circ}C$  was observed due to evaporation of adsorbed water molecules from alumina surface and the steady weight loss of  $\sim 13\%$  up to  $400$   $^{\circ}C$  for the condensation and further crystallization of  $Al_2O_3$  material. This result suggested considerably good thermal stability of the mesoporous  $\gamma$ - $Al_2O_3$  material.

### 3.6. Surface acidity and basicity measurements

In order to investigate the presence of surface acidic and basic sites of mesoporous  $\gamma$ - $Al_2O_3$  material, temperature program desorption analysis of ammonia and carbon dioxide i.e.  $NH_3$ -TPD and  $CO_2$ -TPD have been carried out. The results of the  $NH_3$ -TPD and  $CO_2$ -TPD experiments are shown in Fig. 5A and B, respectively. As seen from Fig. 5A the material exhibits three types of acidity i.e. weak, medium and strong with  $NH_3$  desorption peak maximas at  $110$ ,  $315$  and  $548$   $^{\circ}C$  temperature. The total surface acidity estimated from this  $NH_3$ -TPD plot was  $1.47$   $mmol\ g^{-1}$ . Similarly, Fig. 5B represents the  $CO_2$ -TPD of MPA-1 material where the three distinct peaks appeared and these are assigned to the presence of weak, medium and strong basic sites with peak maximums at temperatures  $97$ ,  $352$  and  $550$   $^{\circ}C$ . From Fig. 5B, the total surface basicity of the material was estimated as  $1.11$   $mmol\ g^{-1}$ . The high surface acidic and basic sites present in the mesoporous  $\gamma$ - $Al_2O_3$  material have motivated us to perform the liquid phase acid-base

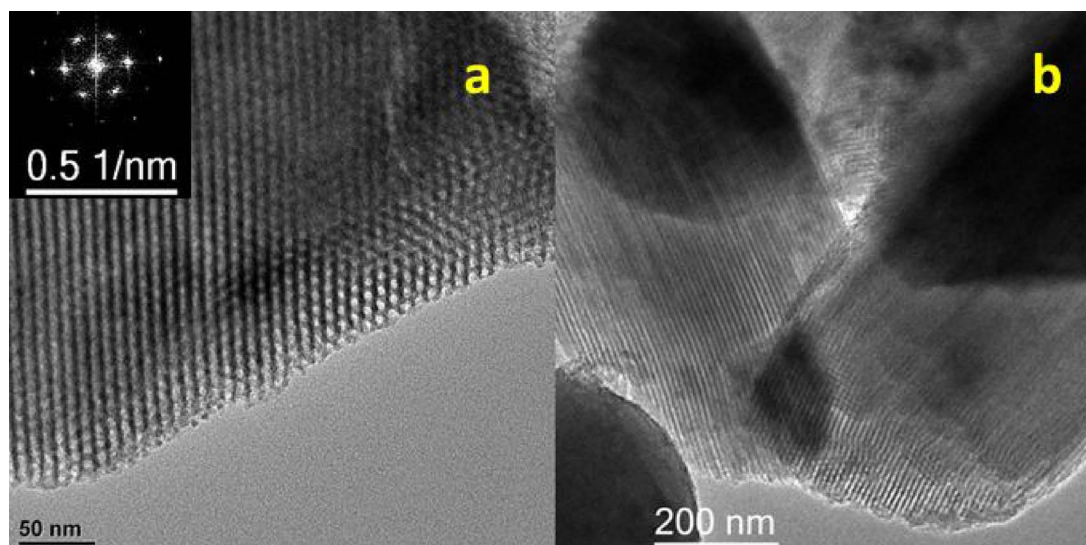


Fig. 4. UHR-TEM images of MPA-1.

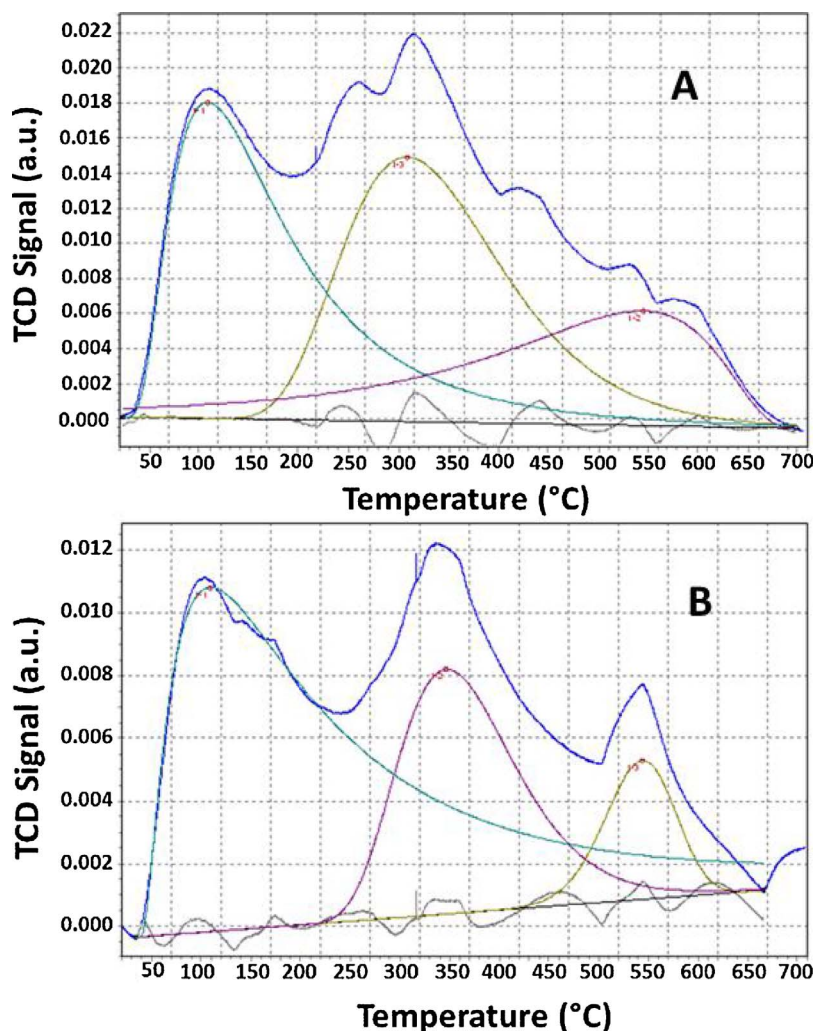


Fig. 5. The NH<sub>3</sub> (A) and CO<sub>2</sub> (B) TPD profile diagrams of MPA-1 material.

tandem catalytic condensation reaction.

### 3.7. Catalysis

Owing to its high surface acidic and basic sites at the mesoporous alumina surface MPA-1 material could be employed as a heterogeneous amphoteric catalyst for tandem organic transformation reaction. To explore the catalytic activity of the MPA-1 we have carried out the C–C bond forming Knoevenagel condensation reaction using various electron-donating or withdrawing groups present in substituted aromatic aldehydes and active methylene group containing malononitrile for the synthesis of substituted benzylidene-malononitrile products at room temperature. Since, coumarin-3-carboxylic acid is biologically active compound we have performed the Knoevenagel condensation reaction using salicylaldehyde and malononitrile to obtain 2-(2-hydroxybenzylidene)-malononitrile as an intermediate product, which was subjected for further acid hydrolysis for synthesis of coumarin-3-carboxylic acid. Furthermore, a wide range of substituted  $\alpha,\beta$ -unsaturated compounds are synthesized using MPA-1 as catalyst and this results are enlisted in Table 1. Also, the schematic representation for the synthesis of coumarin-3-carboxylic acid has been shown in Scheme 2. Further, the mesoporous  $\gamma$ -Al<sub>2</sub>O<sub>3</sub> material calcined at 1000 °C MPA-2 showed almost equal activity to MPA-1 for the synthesis of 2-(4-chlorobenzylidene)-malononitrile under similar reaction conditions (Table 1, entry 7).

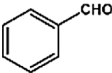
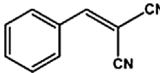
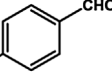
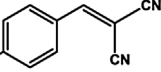
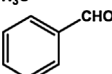
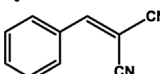
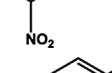
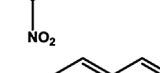
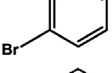
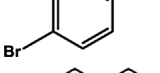
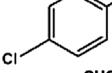
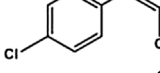
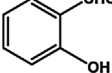
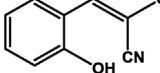
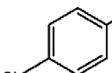
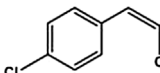
Moreover, for the synthesis of various substituted benzylidene-malononitrile through Knoevenagel condensation reaction some

reaction parameters, like solvents, temperatures etc. also play crucial roles. From the results shown in Table 2 it has been concluded that the reaction is more feasible in absolute ethanol at room temperature for 7 min, where the maximum product yield is obtained to be 98% from *p*-chlorobenzaldehyde. In aqueous medium the product yield was 83% which is much more than that in other two solvents i.e. CH<sub>3</sub>CN and DMF. This result indicates that the reaction is mainly feasible in polar protic solvents. Bigi et al. have synthesized benzylidene-malononitriles in high yields (84–98%) using water as solvent at 65 °C for 1 h without adding any catalyst during reaction [50]. A possible mechanistic pathway for formation of coumarin-3-carboxylic acids has been outlined in Scheme 3. Due to the amphoteric nature, alumina plays more active role in providing the substantial surface acidity and basicity [51]. In this proposed mechanism mesoporous alumina surface can simultaneously activate the carbonyl oxygen as well as active methylene group due to its amphoteric nature. The reaction can proceed smoothly through the formation of six member cyclic transition state, which could be the driving force for fast reaction rate. Further, the resulting di-cyano product was subjected for acid hydrolysis and cyclization to form the coumarin-3-carboxylic acid in the presence of sulfuric acid at 50 °C.

### 3.8. Reusability test

To check the recyclability of the catalyst we have performed Knoevenagel condensation reaction using *p*-chlorobenzaldehyde and malononitrile at room temperature for 7 min over MPA-1 for 6th

**Table 1**  
Knoevenagel condensation between various aldehydes and malononitrile catalyzed by mesoporous  $\gamma$ -Al<sub>2</sub>O<sub>3</sub> at room temperature.<sup>a</sup>

Entry	Substrates	Time (min)	Products	Yields (%)
1.		13		98
2.		15		98
3.		8		99
4.		7		98
5.		7		98
6.		25		95
7. <sup>b</sup>		7		98
				98

<sup>a</sup> Reaction conditions: aldehyde (1 mmol), malononitrile (1.1 mmol), catalyst (10 mg), solvent (absolute ethanol), reaction temperature = room temperature.

<sup>b</sup> MPA-2 was used as catalyst.

reaction cycle. After completion of first reaction cycle the solid MPA-1 catalyst has been recovered from the reaction mixture and dried it in air oven at 100 °C for second reaction cycle. No fresh catalyst has been added to compensate the very little amount loss of catalyst after each reaction cycle. However, it is noticed from Fig. 6 the reused MPA-1 catalyst exhibits excellent product yield up to sixth reaction cycle without significant loss of product yield (ca. 2%). This result suggests that this material has huge potential for the C–C bond formation via Knoevenagel condensation reaction.

#### 4. Conclusion

Our experimental results suggested that we can synthesize biologically active value added important coumarin derivatives via Knoevenagel condensation reaction using 2D-hexagonally ordered mesoporous  $\gamma$ -Al<sub>2</sub>O<sub>3</sub> as an amphoteric heterogeneous catalyst. Strong Lewis acidic and basic sites present at the mesoporous  $\gamma$ -Al<sub>2</sub>O<sub>3</sub> surface and its high specific surface area are the main driving force for catalyzing the Knoevenagel condensation reactions with excellent product yields (~98%). The acidic and basic nature along with the ordered mesoporosity of  $\gamma$ -Al<sub>2</sub>O<sub>3</sub> reported herein can be very useful to explore its potential applications in several other organic transformations and

**Table 2**

Effect of solvents and reaction temperatures for synthesis of  $\alpha,\beta$ -unsaturated di-cyano products from *p*-chlorobenzaldehyde as a representative substrate using  $\gamma$ -Al<sub>2</sub>O<sub>3</sub> catalyst<sup>a</sup>.

Entry	Catalysts	Solvents	Temperature (°C)	Time (min)	Yield (%)
1.	MPA-1	H <sub>2</sub> O	25	30	83
2.	MPA-1	CH <sub>3</sub> CN	25	120	15
3.	MPA-1	CH <sub>3</sub> CN	50	120	20
4.	MPA-1	EtOH	25	7	98
5.	MPA-1	EtOH	50	20	98
<sup>b</sup> 6.	Basic Al <sub>2</sub> O <sub>3</sub>	EtOH	25	20	96
7.	MPA-1	DMF	25	120	50
8.	No catalyst	EtOH	25	180	92

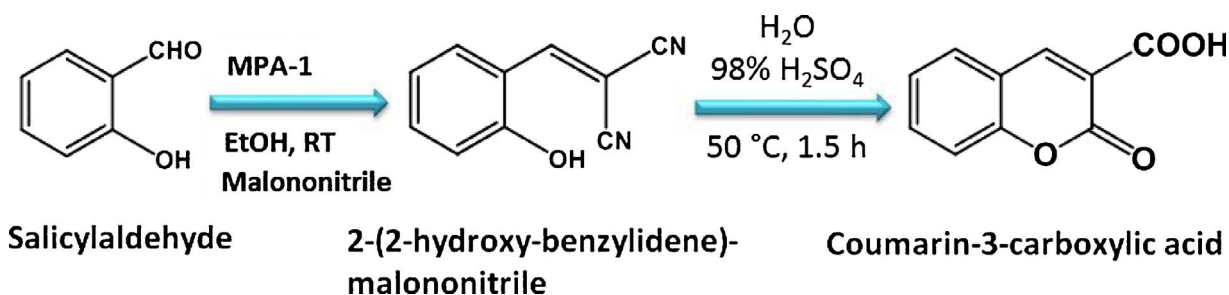
<sup>a</sup>Reaction condition: aldehyde (1 mmol), malononitrile (1.1 mmol), MPA-1 catalyst (10 mg).

<sup>b</sup> Reaction condition: aldehyde (1 mmol), malononitrile (1.1 mmol), Basic alumina catalyst (10 mg).

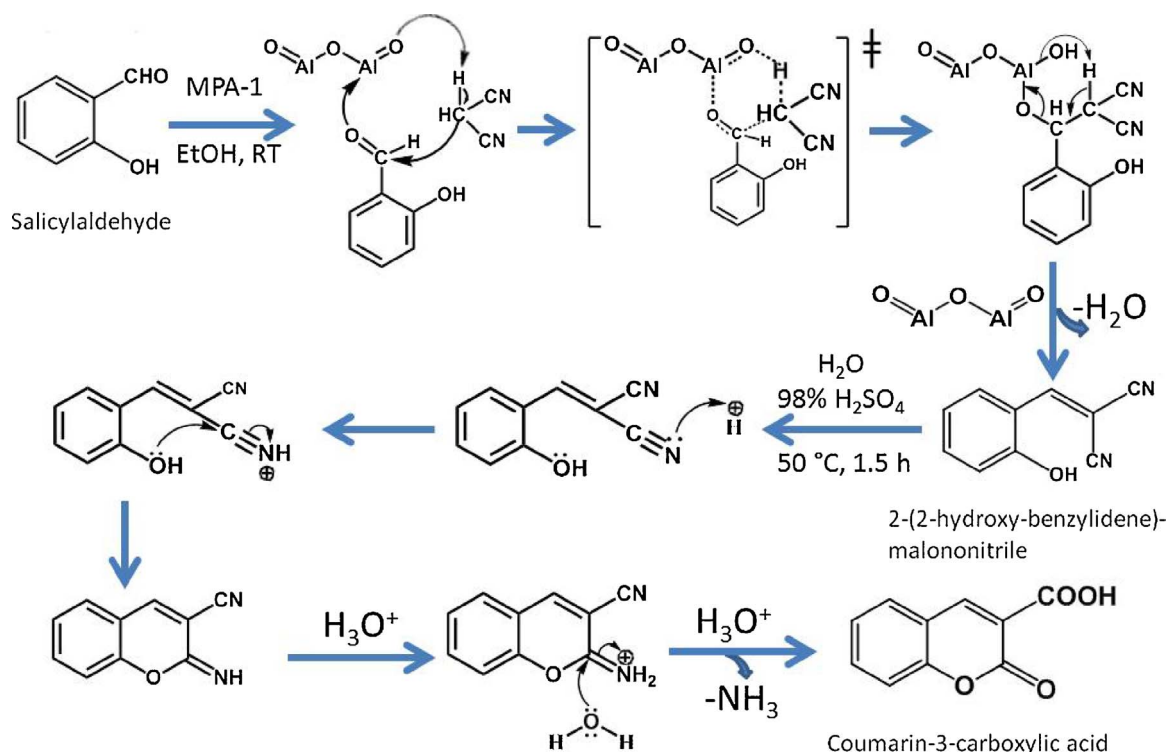
bright future in sustainable catalysis.

#### Acknowledgements

PB wishes to thank CSIR, New Delhi for their senior research



**Scheme 2.** Schematic outline for synthesis of coumarin-3-carboxylic acid.



Scheme 3. Possible mechanistic pathway for the synthesis of coumarin-3-carboxylic acid.  $\gamma$ - $\text{Al}_2\text{O}_3$  is presented as  $\text{O}=\text{Al}-\text{O}-\text{Al}=\text{O}$  for simplicity.

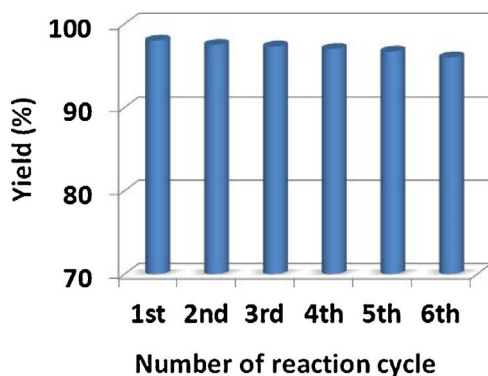


Fig. 6. Recycling efficiency for the Knoevenagel condensation reaction between *p*-chlorobenzaldehyde and malononitrile over MPA-1.

fellowship. UK wishes to thank DST-SERB for NPDP project grant. AB wishes to thank DST, New Delhi for financial support through the DST-ASRT, Indo-Egypt international project grant.

#### Appendix A. Supplementary data

Supplementary data associated with this article can be found, in the online version, at <http://dx.doi.org/10.1016/j.mcat.2018.01.019>.

#### References

- M. Zahradnik, *The Production and Application of Fluorescent Brightening Agents*, Wiley & Sons, Chichester, 1992.
- P. Frosch, J.D. Johansen, T. Menne, C. Pirker, S.C. Rastogi, K.E. Andersen, M. Bruze, A. Goossens, J. Lepoittevin, I.R. White, *Contact Dermatitis* 47 (2002) 279–287.
- M.D. Moreira, M.C. Picanço, L.C.D.A. Barbosa, R.N.C. Guedes, M.R. Campos, G.A. Silva, J.C. Martins, *Pesqui. Agropecu. Bras.* 42 (2007) 909–915.
- T. Felbeck, S. Moss, A.M.P. Botas, M.M. Lezhnina, R.A.S. Ferreira, L.D. Carlos, U.H. Kynast, *Colloids Surf. B Biointerfaces* 157 (2017) 373–380.
- Y.-T. Chen, C.-Y. Lin, G.-H. Lee, M.-L. Ho, *CrystEngComm* 17 (2015) 2129–2140.
- R. Banerjee, S. Mondal, P. Purkayastha, *RSC Adv.* 6 (2016) 105347–105349.
- P. Gonzalez, K. Pota, L. Turan, V.C.P. da Costa, G.R. Akkaraju, K.N. Green, *ACS Chem. Neurosci.* (2017), <http://dx.doi.org/10.1021/acscemneuro.7b00184>.
- N. Hamdi, R. Medyouni, A. Sulaiman Al-Ayed, L. Mansour, A. Romerosa, J. *Heterocycl. Chem.* 54 (2017) 2342–2351.
- S.R. Kulkarni, P.F. Khatwani, V. Gurale, *Int. J. Pharma. Bio. Sci.* 7 (2016) 315–326.
- H. Zhao, N. Neamati, H. Hong, A. Mazumder, S. Wang, S. Sunder, G.W. Milne, Y. Pommier, T.R. Burke, *J. Med. Chem.* 40 (1997) 242–249.
- P. Srivastava, V.K. Vyas, B. Variya, P. Patel, G. Qureshi, M. Ghate, *Bioorg. Chem.* 67 (2016) 130–138.
- L.-M. Herzig, I. Elamri, H. Schwalbe, J. Wachtveitl, *Phys. Chem. Chem. Phys.* 19 (2017) 14835–14844.
- T.F. Stefanello, B. Couturaud, A. Szarpak-Jankowska, D. Fournier, B. Louage, F.P. Garcia, C.V. Nakamura, B.G.D. Geest, P. Woisel, B. van der Sanden, R. Auzély-Velty, *Nanoscale* 9 (2017) 12150–12162.
- A.A. El-Bindary, N. Hassan, M.A. El-Affify, *J. Mol. Liq.* 242 (2017) 213–228.
- L.A. Singer, N.P. Kong, *J. Am. Chem. Soc.* 88 (1966) 5213–5219.
- A.M. Song, X.B. Wang, K.S. Lam, *Tetrahedron Lett.* 41 (2003) 1775–1777.
- O.S. Detistov, S.S. Panda, P.J. Steel, A.M. Abdullah, C.D. Hall, A.R. Katritzky, *Synlett* 25 (2014) 2654–2660.
- D. Jonsson, M. Erlandsson, A. Unden, *Tetrahedron Lett.* 42 (2001) 6953–6956.
- L. Bonsignore, F. Cottiglia, S.M. Lavagna, G. Loy, D. Secci, *Heterocycles* 50 (1999) 469–478.
- H. Safdari, A. Neshani, A. Sadeghian, M. Ebrahimi, M. Iranshahi, H. Sadeghian, *J. Antibiot.* 67 (2014) 373–377.
- R.L. Shriner, *Org. React.* 1 (1942) 1–37.
- H. von Pechmann, C. Duisberg, *Chem. Ber.* 37 (1884) 929–936.
- I. Yavari, R.H. Shoar, A. Zonouzi, *Tetrahedron Lett.* 39 (1998) 2391–2392.
- M. Maheswara, V. Siddaiah, G.L.V. Damu, Y.K. Rao, C.V. Rao, *J. Mol. Catal. A: Chem.* 255 (2006) 49–52.
- J. Mondal, A. Modak, A. Bhaumik, *J. Mol. Catal. A: Chem.* 335 (2011) 236–241.
- M. Stekrova, P. Maki-Arvela, N. Kumar, E. Behraves, A. Aho, Q. Balme, K.P. Volcho, N.F. Salakhutdinov, D.Y. Murzin, *J. Mol. Catal. A: Chem.* 410 (2015) 260–270.
- L.F. Tietze, *Chem. Rev.* 96 (1996) 15–136.
- G. Brufola, F. Fringuelli, O. Piermatti, F. Pizzo, *Heterocycles* 45 (1997) 1715–1721.
- S.A.-E. Ayoubi, F. Texier-Boullet, J. Hamelin, *Synthesis* (1994) 258–260.
- T.J. Schwartz, S.D. Lyman, A.H. Motagamwala, M.A. Mellmer, J.A. Dumesic, *ACS Catal.* 6 (2016) 2047–2054.
- H. Wang, W.-H. Fang, X. Chen, *J. Org. Chem.* 81 (2016) 7093–7101.
- Y. Zhang, A. Zhu, Q. Li, L. Li, Y. Zhao, J. Wang, *RSC Adv.* 4 (2014) 22946–22950.
- G. Brahmachari, *ACS Sustainable Chem. Eng.* 3 (2015) 2350–2358.
- B.M. Reddy, P.M. Sreekanth, Y. Yamada, T. Kobayashi, *J. Mol. Catal. A: Chem.* 227 (2005) 81–89.
- D. Shee, A. Sayari, *Appl. Catal. A: Gen.* 389 (2010) 155–164.
- A.V.H. Soares, J.B. Salazar, D.D. Falcão, F.A. Vasconcellos, R.J. Davis, F.B. Passos, *J. Mol. Catal. A: Chem.* 415 (2016) 27–36.
- G.W. Kabalka, R.M. Pagni, *Tetrahedron* 53 (1997) 7999–8065.
- S.E. Tung, E. Mcininch, *J. Catal.* 3 (1964) 229–238.

- [39] A.K. Patra, A. Dutta, A. Bhaumik, J. Hazard. Mater. 201 (2012) 170–177.
- [40] S. Karnjanakom, A. Bayu, X.G. Hao, S. Kongparakul, C. Samart, A. Abudula, G.Q. Guan, J. Mol. Catal. A: Chem. 421 (2016) 235–244.
- [41] K. Niesz, P. Yang, G.A. Somorjai, Chem. Commun. (2005) 1986–1987.
- [42] Q. Liu, A.Q. Wang, X.D. Wang, T. Zhang, Chem. Mater. 18 (2006) 5153–5155.
- [43] J. Lian, J. Ma, X. Duan, T. Kim, H. Li, W. Zheng, Chem. Commun. 46 (2010) 2650–2652.
- [44] J. Wei, Y. Ren, W. Luo, Z. Sun, X. Cheng, Y. Li, Y. Deng, A.A. Elzatahry, D. Al-Dahyan, D. Zhao, Chem. Mater. 29 (2017) 2211–2217.
- [45] C. Weinberger, Z. Chen, W. Birnbaum, D. Kuckling, M. Tiemann, Eur. J. Inorg. Chem. (2017) 1026–1031.
- [46] Q. Yuan, A.-X. Yin, C. Luo, L.-D. Sun, Y.-W. Zhang, W.-T. Duan, H.-C. Liu, C.-H. Yan, J. Am. Chem. Soc. 130 (2008) 3465–3472.
- [47] P. Bhanja, R. Gomes, L. Satyanarayana, A. Bhaumik, J. Mol. Catal. A: Chem. 415 (2016) 104–112.
- [48] A. Dutta, D. Gupta, A.K. Patra, B. Saha, A. Bhaumik, ChemSusChem 7 (2014) 925–933.
- [49] P. Paul, P. Bhanja, N. Salam, U. Mandi, A. Bhaumik, S.M. Alam, S.M. Islam, J. Colloid Interface Sci. 493 (2017) 206–217.
- [50] F. Bigi, M.L. Conforti, R. Maggi, A. Piccinno, G. Sartori, Green Chem. 2 (2000) 101–103.
- [51] M.E. Potter, K.M. Cho, J.J. Lee, C.W. Jones, ChemSusChem 10 (2017) 2192–2201.